Article

Effects of Macromolecular Crowding on the Structure of a Protein Complex: A Small-Angle Scattering Study of Superoxide Dismutase

Ajith Rajapaksha,[1] Christopher B. Stanley,[2] and Brian A. Todd[1,*]
[1]Department of Physics and Astronomy, Purdue University, West Lafayette, Indiana; and [2]Biology and Soft Matter Division, Oak Ridge National Laboratory, Oak Ridge, Tennessee

ABSTRACT Macromolecular crowding can alter the structure and function of biological macromolecules. We used small-angle scattering to measure the effects of macromolecular crowding on the size of a protein complex, SOD (superoxide dismutase). Crowding was induced using 400 MW PEG (polyethylene glycol),TEG (triethylene glycol), α-MG (methyl-α-glucoside), and TMAO (trimethylamine *n*-oxide). Parallel small-angle neutron scattering and small-angle x-ray scattering allowed us to unambiguously attribute apparent changes in radius of gyration to changes in the structure of SOD. For a 40% PEG solution, we find that the volume of SOD was reduced by 9%. Considering the osmotic pressure due to PEG, this deformation corresponds to a highly compressible structure. Small-angle x-ray scattering done in the presence of TEG suggests that for further deformation—beyond a 9% decrease in volume—the resistance to deformation may increase dramatically.

INTRODUCTION

Biological environments contain between 7 and 40% macromolecules by volume (1,2). This reduces the available aqueous volume and elevates the osmotic pressure relative to pure water. Consequently, biological macromolecules in their native environments tend to adopt more compact and dehydrated conformations than those in vitro. This effect is referred to as "macromolecular crowding" (1,3) and also as "osmotic stress" (4).

There have been relatively few studies to determine how macromolecular crowding influences the structure of multimeric protein complexes (5). In this work, we used small-angle scattering (SAS), to measure changes in the structure of a protein complex as a function of macromolecular crowding. In contrast to previous studies that looked at how macromolecular crowding shifts the equilibrium between distinct conformational states (6–8), our work examines subtle crowding-induced structural changes of a single stable conformation. Crowding tends to compress macromolecular structures, and in this work we measure the compressibility modulus of a protein complex. To our knowledge, this is the first measurement of the osmotic compressibility for a protein complex.

A major difficulty in using SAS to measure the effects of macromolecular crowding on protein structure is that crowding agents contribute to the measured scattering profile. Additional scattering from the bulk solution can be removed by background subtraction (9,10). However, many proteins are surrounded by a hydration layer whose composition differs both from the bulk solution and from the protein (11,12). Because the scattering length density (SLD) of the bulk solution changes as crowding agents are added, the relative contrast of the hydration layer and the protein with respect to the bulk change. Consequently, changes in the scattering profile as crowding agents added to the solution can reflect either changes in protein structure or changes in relative scattering contrast (8,13). In this work, we adapted the technique of Svergun et al. (12), which exploits the different contrast mechanisms of small-angle x-ray scattering (SAXS) and small-angle neutron scattering (SANS) to independently assess the contribution from the hydration layer. This allowed us to unambiguously interpret our scattering experiments in terms of structural changes of the protein complex under study.

The protein complex that we chose for our study is the homodimeric complex of SOD (superoxide dismutase). We selected a homodimeric protein complex because it is the simplest possible protein complex. Consequently, structural modeling of our experimental data would be highly constrained. SOD was selected from a bioinformatic survey of the hydration of protein-protein interfaces (14). Of the 161 protein complexes surveyed, SOD was found to have the largest number of crystallographically observed waters per unit area of interface; that is, the dimeric interface of SOD is unusually wet. Because one of the effects of macromolecular crowding is to dehydrate the water-filled cavities of proteins (4), SOD might be expected to be particularly sensitive to macromolecular crowding. Indeed, we find that the volume of SOD observed in buffer decreased by 9% upon adding 40 vol % of a macromolecular crowding agent. This indicates that the structure of protein complexes can be quite sensitive to macromolecular crowding.

Submitted November 10, 2014, and accepted for publication December 29, 2014.

*Correspondence: batodd@purdue.edu

Editor: Lois Pollack.

0006-3495/15/02/0967/8 $2.00

http://dx.doi.org/10.1016/j.bpj.2014.12.046

MATERIALS AND METHODS

Materials

SOD (superoxide dismutase, lyophilized, Cat. No. S5389); PEG (polyethylene glycol, Cat. No. 202398) of an average molecular mass of 400 Da; TEG (triethylene glycol, Cat. No. 95126); α-MG (methyl-α-D-glucopyranoside, Cat. No. M9376); and TMAO (trimethylamine-*n*-oxide, Cat. No. T0514) were purchased from Sigma-Aldrich (St. Louis, MO). dPEG (deuterated PEG, 100%) for SANS experiments was purchased from Polymer Source (Montreal, Canada; Cat. No. P9878A dPEO2OD). D_2O (deuterium oxide, 100 atom %) was purchased from Fisher Scientific (Pittsburgh, PA; Cat. No. 184761000). An SOD activity assay was purchased from Cell Biolabs (San Diego, CA; Cat. No. STA-340). All materials were used without further purification.

Material storage and preparation

SOD stock solutions were prepared at 20 mg/mL concentration and stored at −20°C. Assay solutions and SAXS samples were prepared in Milli-Q deionized water (Millipore, Billerica, MA). SANS samples were prepared in D_2O. All solutions were buffered at pH 7.5 in 0.1 M potassium phosphate buffer. In the preparation of samples that contained both SOD and PEG, SOD was added from the initial stock to buffer solutions prepared with appropriate volume fractions of PEG. The same procedure, as for PEG, was followed for other solutes. All experiments were performed at laboratory temperature and atmospheric pressure.

SOD activity assay

SOD catalyzes the conversion of super-oxide anions (O_2^-) into molecular oxygen in biological systems (15,16). SOD assays typically use an additional enzyme to generate O_2^- and measure the ability of SOD to reduce O_2^- in the solution (17). We used a commercial SOD activity assay where XOD (xanthine oxidase) generates O_2^- (Cell Biolabs). Chromagen present in the solution combines with O_2^- to produce an increase in absorption at 491 nm (OD_{491}). Colorimetric measurements were made using a Varian UV-Vis spectrometer (Cary, NC) at room temperature in clear plastic UV-Vis cuvettes purchased from SpectrEcology (Jasper, GA; Cat. No. 759220).

Fig. 1 shows typical data indicating the evolution of OD_{491} as a function of time. Concentrations of SOD are conventionally given in units/mL where an SOD unit is defined as the amount of SOD required to decrease the

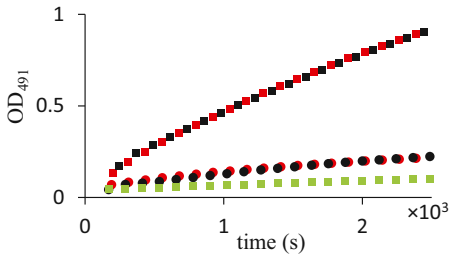

FIGURE 1 Optical absorption at 491 nm (OD_{491}) for an SOD activity assay where SOD reduces O_2^- produced by XOD. (*Red*) Standard behavior of the assay in absence of SOD (*red squares*) and in the presence of 10 U/mL SOD (*red circles*). In a 70% PEG solution containing no SOD, OD_{491} is decreased (*green squares*). When the assay was modified by fivefold increase in XOD concentration (*black squares*), the assay displayed similar activity to the standard assay conditions (*black squares* similar to *red squares*). In 70% PEG with fivefold increased XOD, addition of 10 U/mL SOD (*black circles*) reduced the OD_{491} to a similar level as in the standard assay (*black circles* similar to *red circles*). To see this figure in color, go online.

reduction of cytochrome *c* by 50% in a xanthine/xanthine-oxidase coupled system, at pH 7.8 and at 25°C (18). The important parameter taken from each time course was the initial rate of increase in OD_{491}, *r*. In the absence of SOD, *r* is maximal (*red squares*). Upon addition of SOD (e.g., 10 units/mL), *r* is reduced (*red circles*). The %inhibition is defined as

$$\%\text{inhibition} = \frac{r_{\text{blank}} - r_{\text{SOD}}}{r_{\text{blank}}} \times 100, \qquad (1)$$

where r_{blank} is the rate of increase of OD_{491} measured in the absence of SOD and r_{SOD} is the rate of increase of OD_{491} measured at a particular SOD concentration.

We sought to use the SOD activity assay to determine whether SOD retained its enzymatic activity at high PEG concentration. However, the XOD used to generate O_2^- in the assay could also be sensitive to the presence of PEG. Consequently, we first measured XOD activity in the presence of 70% PEG with no SOD present ("%PEG" refers to the % of PEG by volume). XOD showed reduced activity in 70% PEG (Fig. 1, *green squares*). Increasing the concentration of XOD used in the assay by a factor of 5 recovered the same activity in 70% PEG (Fig. 1, *black squares*) as was seen under standard assay conditions (Fig. 1, *red squares*). Consequently, for all measurements in the presence of 70% PEG, we used fivefold higher concentration of XOD than is used in the standard assay (19). Upon addition of SOD (e.g., 10 units/mL) to a solution with fivefold higher XOD in 70% PEG, the rate of increase of OD_{491} was reduced (Fig. 1, *black circles*) to similar levels seen in the absence of PEG (Fig. 1, *red circles*).

Small-angle scattering

SANS experiments were performed on the extended *q*-range SANS (EQ-SANS, BL-6) beam line at the Spallation Neutron Source (Oak Ridge National Laboratory, Oak Ridge, TN). In 60-Hz operation mode, a 4-m sample-to-detector distance was used to obtain the relevant wavevector transfer, $q = 4\pi\sin(\theta)/\lambda$, where 2θ and λ, respectively, are the scattering angle and the wavelength. At 4-m sample-to-detector distance 2.5–6.1 Å wavelength band was utilized scanning through the *q* range from 0.01 to 0.40 $Å^{-1}$.

SAXS experiments were performed at beamline 12ID-B at the Advanced Photon Sources facility (Argonne National Laboratory, Lemont, IL). The value λ, for x-ray radiation, was set as 0.886 Å. Scattered x-ray intensities were measured using a Pilatus 2M detector (DECTRIS, Baden, Switzerland). A sample-to-detector distance of 4 m was set such that the detecting range of momentum transfer was 0.006–0.5 $Å^{-1}$.

The solutions prepared for scattering experiments were subjected to ultracentrifugation at 20,000*g* for 5 min before placing in the neutron or x-ray beam. Ultracentrifuged solutions did not produce any visible sediment. However, ultracentrifugation of SANS samples prepared with dPEG appeared to have a very thin accumulation on the surface of the solution. This may be due to a small amount of impurities gleaned from dPEG synthesis. Solutions for the neutron beam were obtained from the bottom of the solution avoiding these accumulations. In SANS, the additional scattering from PEG was minimized using dPEG in D_2O. This also reduced incoherent scattering.

In SANS experiments, samples were loaded into 1-mm pathlength circular-shaped quartz cuvettes (Hellma USA, Plainville, NY). Average neutron exposure time was 1 h. Scattered neutrons were detected with a 1 × 1 m, two-dimensional position-sensitive detector with 192 × 256 pixels. Data reduction followed standard procedures using the softwares MANTIDPLOT (20) and PRIMUS (9). The measured scattering intensity was corrected for the detector sensitivity and scattering contribution from the solvent and empty cells, and then placed on absolute scale using a calibrated standard.

In SAXS experiments, a flow cell made of a cylindrical quartz capillary (1.5-mm diameter and 10-μm wall-thickness) was used and the exposure time was set to 1–2 s. For every measurement, the x-ray beam of 0.07 × 0.20 mm^2 was adjusted to pass through the center of the capillary. To obtain

good signal/noise, 60 images were taken for each sample and buffer. The two-dimensional scattering images were converted to one-dimensional SAXS curves through radial averaging after solid angle correction and then normalizing with the intensity of the transmitted x-ray beam, using the software package developed at beamline 12ID-B (Advanced Photon Source).

SOD radius of gyration, R_g was calculated using Guinier plots ($\ln[I(q)$ versus q^2) in the low q region within the limit $q_{max}R_g < 1.3$. Guinier plots were made with the software PRIMUS (9). Pair distance distribution functions, $P(r)$, were made using the software GNOM (21). In the process of producing $P(r)$, the maximum linear dimension, D_{max}, was chosen iteratively for each background-subtracted data set, such that the $P(r)$ curves approach zero at D_{max} in a smooth concave manner (10,22).

Small-angle scattering predictions were obtained using the software CRYSON (12). The protein structure PDB 1ISA (23) was obtained from the Protein Data Bank (www.rcsb.org).

Osmotic pressure measurements

Osmotic pressure measurements were made using a Vapro 5520 vapor pressure osmometer (Wescor, Logan, UT). Osmolalities measured by the osmometer were converted into osmotic pressure using $\Pi = [Osmol]\rho RT$, where Π is osmotic pressure, $[Osmol]$ is the osmolality, ρ is the density of water, R is the gas constant, and T is the absolute temperature (24,25). The value $\Delta\Pi$ is the osmotic pressure in excess of the buffer solution $\Delta\Pi = \Pi - \Pi_0$, where Π_0 is the osmotic pressure of the buffer in the absence of solute.

RESULTS

Biochemical activity of SOD in crowded solutions

A commercial SOD activity assay was used to verify that SOD retains its enzymatic activity in the presence of a high concentration of PEG. Fig. 2 compares SOD activity in standard buffer (*green diamonds*) and SOD activity in 70% PEG (*red triangles*). The concentration of XOD in 70% PEG was increased fivefold to compensate for the effects of PEG on XOD, as described in Materials and Methods. SOD activity in 70% PEG is indistinguishable from the activity in standard buffer, indicating that SOD retains its enzymatic activity at 70% PEG.

Small-angle scattering of SOD

SANS and SAXS were used to measure the size of SOD. In Fig. 3, the scattering intensity versus scattering vector, $I(q)$ versus q, is plotted for SOD in dilute buffer as measured by SANS (*red triangles*) and SAXS (*green diamonds*) and, for the scattering predicted by the software CRYSON (12) (*yellow curve*), for a crystal structure of the SOD dimer (23). The SANS and SAXS data, as well as the predicted scattering for the crystal structure, are identical to within the experimental uncertainty. This indicates that SOD has similar structures under the conditions of the SANS (e.g., D_2O) and SAXS (e.g., H_2O) experiments and that this structure closely matches the structure of SOD measured by x-ray crystallography (23).

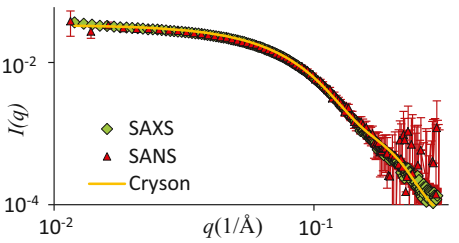

FIGURE 3 SAS for SOD obtained by SAXS (*green diamonds*) and SANS (*red triangles*) in the absence of a crowding agent. (*Yellow curve*) Predicted scattering using the software CRYSON for an SOD crystal structure (12,23). All three curves are identical, indicating that the SOD structure is identical under both SANS and SAXS conditions and that this structure is similar to the crystal structure. To see this figure in color, go online.

PEG was added to solutions to determine how crowding alters the structure of the SOD dimer. Fig. 4 shows SAXS data obtained in dilute solution (*green diamonds*) and in solution containing 40% PEG (*red circles*). If PEG had induced aggregation of SOD, then we would expect increased scattered intensity at low q. To the contrary, the scattered intensity at low q decreased in the presence of PEG. The data in Fig. 4 and similar data for different PEG concentrations were transformed into Guinier plots (26,27) to obtain apparent R_g as a function of PEG concentration.

Fig. 5 shows Guinier plots for SAXS data in the absence of PEG (*green diamonds*) and in 40% PEG (*red circles*). R_g^2 value is proportional to the slope of the Guinier plot (indicated by *lines*). The slope for SOD in 40% PEG is significantly smaller than the slope in the absence of PEG (p-value $= 4.3 \times 10^{-9}$). This indicates that crowding due to PEG decreases the apparent R_g value of SOD. Scattering

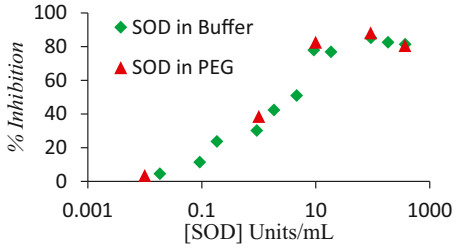

FIGURE 2 The activity of SOD was measured under standard conditions (*green diamonds*) and in the presence of 70% PEG (*red triangles*). The activity of SOD in 70% PEG was indistinguishable from its activity in buffer. To see this figure in color, go online.

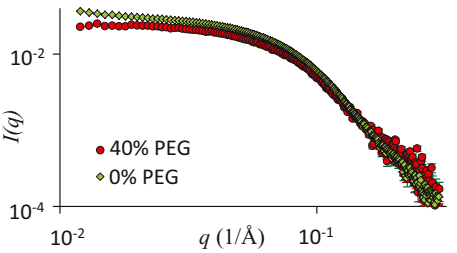

FIGURE 4 SAXS of SOD in buffer (*green diamonds*) and 40% PEG (*red circles*). In 40% PEG, scattering from SOD decreased in the low q region. To see this figure in color, go online.

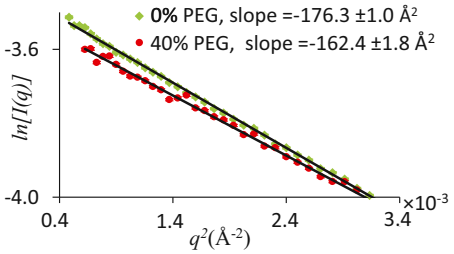

FIGURE 5 Guinier plots for SAXS of SOD in 0% PEG (*green*) and 40% PEG (*red*). The slope of the Guinier plot is proportional to the R_g^2 of the scattering object. In the presence of PEG, the slope of the Guinier plot decreased, indicating a decrease in the apparent R_g in 40% PEG. To see this figure in color, go online.

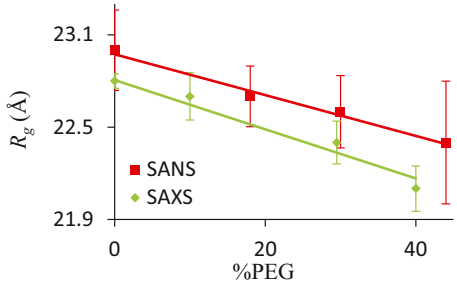

FIGURE 7 R_g measured in SANS (*red squares*) and SAXS (*green diamonds*) as a function of the %PEG. In both SANS and SAXS, the R_g decreased with increased %PEG. (*Solid curves*) Best fit to lines. To see this figure in color, go online.

data were transformed to obtain pair distance distribution functions, $P(r)$ (27,28). Fig. 6 shows $P(r)$ produced from SAXS data for SOD in dilute buffer (*green*) and in 40% PEG solution (*red*). R_g values were calculated from $P(r)$ to be 23.8 Å for SOD in buffer and 22.5 Å for SOD in 40% PEG. The decrease in the R_g measured from $P(r)$ upon addition of PEG is consistent with the decrease in the slopes obtained from Guinier plots (Fig. 5).

SANS and SAXS data were obtained for SOD over a range of PEG concentrations. R_g values were obtained via Guinier plots identical to those shown in Fig. 5. In Fig. 7, R_g measured in SANS (*red squares*) and SAXS (*green diamonds*) are shown as a function of PEG concentration. Both sets of data show a decrease in R_g with increased PEG concentration. The downward trends in SANS and SAXS data can be fitted to straight lines with the slopes $(-1.33 \pm 0.94) \times 10^{-2}$ Å/%PEG and $(-1.60 \pm 0.32) \times 10^{-2}$ Å/% PEG, respectively.

Effects of altered scattering contrast on R_g

Some proteins are surrounded by a layer of pure water that differs from bulk solution (11,12,29,30). This hydration layer may have an SLD that differs from bulk solution and may therefore contribute scattering, in addition to the scattering from the protein. This additional scattering could cause the R_g measured in a Guinier plot to differ from the

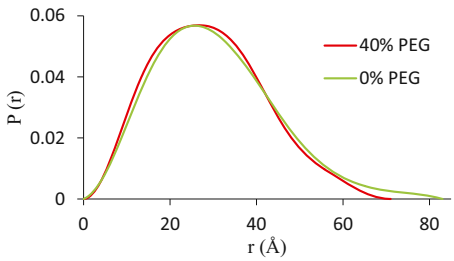

FIGURE 6 Pair distance distribution functions, $P(r)$ for SAXS of SOD in 0% PEG (*green*) and 40% PEG (*red*). R_g values calculated from $P(r)$ are 23.8 Å for SOD in 0% PEG and 22.5 Å for SOD in 40% PEG. To see this figure in color, go online.

R_g of the protein (8,12,13). Additionally, if a solute is added to the solution (as in our PEG experiments), the concomitant change in SLD of the bulk solution would change the relative contrast of the hydration layer and the protein. This change in the contrast of the hydration layer could cause the R_g inferred from the Guinier plot to change as a function of solute concentration even when the protein structure remains constant (8,13). It is, therefore, important to consider the potential contribution of a hydration layer to R_g measured in, for instance, Fig. 7.

SAXS and SANS rely on different contrast mechanisms (10,28,31). Consequently, parallel SAXS and SANS experiments provide a direct way to assess the contribution of change in the bulk SLD on measured changes in R_g (12). The SLD for dPEG in SANS experiments is larger than both the SLD of protein and that of the pure D_2O, which would comprise a hydration layer. In contrast, the SLD for PEG in SAXS experiments is intermediate between the SLD of protein and that of pure H_2O. Because of these differences, the change in R_g as PEG is added to solution would be opposite in direction between SANS and SAXS (R_g increases with added dPEG in SANS but decreases for added PEG in SAXS, or, vice versa). This predicted behavior is inconsistent with our experimental results in Fig. 7, where the R_g obtained from both SANS and SAXS decrease with increasing PEG. We, therefore, conclude that changes in R_g measured from Guinier plots (Fig. 7) reflect changes in the R_g of SOD rather than changes in the contrast of a hydration layer with respect to the bulk solution. We elaborate on this argument using a specific example of a core-shell model for the protein and its hydration layer in the Appendix.

SAXS measurements of SOD with different solutes

SAXS experiments, identical to those above with PEG, were performed for SOD in TEG, α-MG, and TMAO. In Fig. 8, R_g of SOD obtained from Guinier plots of SAXS data are plotted as a function of each solute concentration. Similar to what was observed for SOD in PEG (Fig. 7), increased

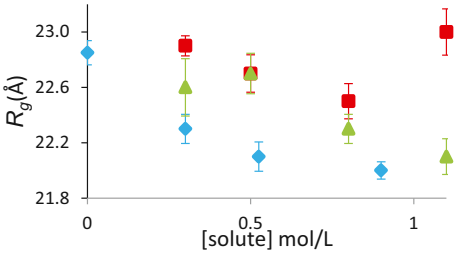

FIGURE 8 R_g of SOD measured in SAXS as a function of the solute concentration in TEG (*blue diamonds*), α-MG (*green triangles*), and TMAO (*red squares*). To see this figure in color, go online.

concentration of these solutes mostly led to decreased R_g of SOD. One instance where the R_g increased with increased solute concentration appears in Fig. 8 for the largest TMAO concentration (*red squares*). We do not know the mechanism by which concentrated TMAO solution differs from the other solutions.

Unlike the data for PEG, we do not have SANS data for the solutes shown in Fig. 8. This was due to the much longer acquisition time required to obtain SANS data. Consequently, for these solutes, we cannot unambiguously rule out the contribution of a hydration layer and changes in SLD to the observed change in R_g. However, the changes in R_g seen in Fig. 8 are similar in magnitude to what was seen in Fig. 7 for PEG in both SANS and SAXS. Of particular interest is the data for TEG (*blue diamonds*) that showed a rapid initial decrease in R_g and plateau at R_g ~ 22 Å. Changes in R_g due to a hydration layer never produce a plateau (elaborated in the Appendix). Hence, it appears likely that the TEG data represents changes in the R_g of SOD rather than an artifact due to a hydration layer. Assuming this to be the case, the plateau observed for TEG would indicate that after a decrease in radius of gyration of ~1 Å, the SOD dimer strongly resists further deformation.

DISCUSSION

Macromolecular crowding can alter the structure and function of biological macromolecules (1,3,32). Previous studies have examined how macromolecular crowding influences protein folding (33), conformational equilibrium (3), substrate binding (34), enzyme kinetics (35,36), and other important properties (37). We have extended these studies by measuring the influence of macromolecular crowding on the size of a multimeric protein complex.

The use of SAS to measure the size of a protein complex faced a number of challenges, including the potential for protein aggregation and artifacts due to a hydration layer surrounding the complex. SAS is very sensitive to aggregation and, by carefully selecting the solution conditions, none was observed. Similar to Svergun et al. (12), we exploited different scattering contrast mechanisms in SAXS and SANS to assess the contribution from any adsorbed water layer. We found that this contribution was negligible and that changes in the radii of gyration observed in Guinier plots could be attributed to changes in the structure of the protein complex.

Previous SAXS studies have observed decreased R_g in the presence of macromolecular crowding and attributed the change to a hydration layer (8,13). Therefore, it appears that some proteins have significant structured water at their surfaces and others, like SOD, do not. Combined SANS and SAXS experiments of the type done here are useful to unambiguously determine the contribution of the hydration layer.

We chose as a model protein complex, the dimer of SOD (15). This dimer has a number of attractive features including availability, easily assessed enzymatic function (38), and a known crystallographic structure (23). SOD is also unusual in that, in a 2005 survey of dimers in the protein data bank, SOD was found to have the largest number of crystallographically observed waters per unit area of the dimer interface; that is, the dimeric interface of SOD is unusually wet (14). Because one of the effects of macromolecular crowding is to dehydrate the water-containing cavities of molecules and macromolecular assemblies (4), SOD may be expected to be particularly sensitive to macromolecular crowding.

We found that at 40% PEG, R_g of SOD decreased by 3% (Fig. 7). It was possible to observe a similar change in the SOD structure through a similar range of concentrations for other solutes as well (Fig. 8). Within the concentration range of our experiments, no solute could reduce the R_g of SOD beyond 4%.

To consider the deformability of SOD implied by these measurements, we plot the volumetric strain, $\Delta V/V_0$ versus change in osmotic pressure due to PEG, $\Delta\Pi$ (Fig. 9). $\Delta V/V_0$ is calculated from the measured R_g, $\Delta V/V_0 = (R_g^3 - R_{g0}^3)/R_{g0}^3$, where $R_{g,0}$ is the R_g of SOD in the absence of PEG. Osmotic pressure was measured as described in the Materials and Methods. Empirically, $\Delta\Pi$ is linearly proportional to $\Delta V/V_0$ with a proportionality constant that is the apparent bulk modulus (*lines* in Fig. 9). Deformations in the SOD structure may be heterogeneous with some regions of the

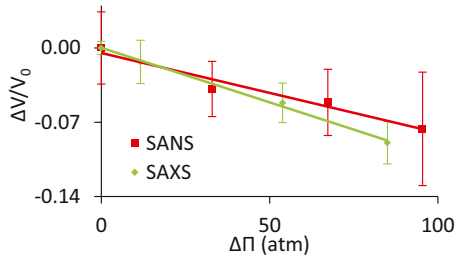

FIGURE 9 Volumetric strain of SOD, $\Delta V/V_0$ versus change in osmotic pressure; $\Delta\Pi$ measured by SAXS (*green diamonds*), and SANS (*red squares*). Both SAXS and SANS display linear relationships between $\Delta V/V_0$ and $\Delta\Pi$. A bulk modulus was estimated from slopes of the regression lines (*solid lines*). To see this figure in color, go online.

complex remaining rigid while others are highly deformable. The apparent bulk modulus gives an average measure of the change in volume caused by a given level of macromolecular crowding.

Estimated bulk moduli of SOD are 0.10 ± 0.02 GPa from SAXS and 0.13 ± 0.1 GPa from SANS. For comparison, measurements of osmotically squeezed collagen assemblies indicate a decrease in interhelical spacing of 2.5 Å for an increase in osmotic pressure of ~100 atm (39). Over this range of pressures, the apparent bulk modulus of self-assembled collagen arrays is 0.03 GPa. This is ~3 times smaller than the bulk modulus for SOD. It is surprising that the compressibilities of self-assembled collagen arrays and SOD are so similar. Collagen monomers in self-assembled collagen arrays are separated by a 5–6.5 Å layer of water (39). In the presence of high molecular-weight osmolytes, there is a thermodynamic driving force for dehydrating the collagen arrays; in effect, water is being squeezed out from a sponge. In contrast, in protein interfaces, many atoms from opposing monomers are in van der Waals contact (23). Thus to first-order, the interface might be thought to be incompressible. However, our measurements show that this is not the case; the compressibility of SOD is, in fact, quite comparable to the compressibility of well-hydrated collagen arrays.

Our measurements indicate how a protein complex decreases in size due to macromolecular crowding. This change in size could result from a number of distinct mechanisms. For example, macromolecular crowding could promote dehydration of the protein interface. Or, macromolecular crowding could cause compaction of protein monomers. It would be difficult using our SAS data alone to differentiate between these two mechanisms. However, because the osmotic work contributed by a solute depends on the volume of water excluding the solute, it may be possible to differentiate dehydration of the dimer interface from compression of the monomers using solutes that are differentially excluded from protein interfaces and the external surfaces of the monomers. We expect the combined SANS and SAXS approach described here to be useful for these and other SAS investigations of macromolecular crowding.

CONCLUSIONS

We used SAS to measure the deformability of a protein complex, SOD, under macromolecular crowding. Parallel SANS and SAXS allowed us to unambiguously attribute apparent changes in R_g to changes in the structure of SOD. For a 40% PEG solution, we find that the volume of SOD was reduced by 9%. Considering the osmotic pressure due to PEG, this deformation corresponds to a compressible structure with a bulk modulus ~0.1 GPa. SAXS done in the presence of TEG suggests that for further deformation—beyond a 9% decrease in volume—the resistance to deformation may increase dramatically.

TABLE 1 Scattering length densities

Term	Neutron (cm^{-2})	X ray (e/nm^3)
ρ_{water}	6.38×10^{10}[a]	334.0
$\rho_{protein}$	3.10×10^{10}	420.0
ρ_{PEG}	7.42×10^{10}[b]	375.0

The ρ-values were calculated with the NIST SLD calculator (41).
[a]SLD of D_2O.
[b]SLD of dPEG.

APPENDIX

Some proteins are surrounded by a layer of pure water that differs from bulk solution (11,12,29,30). If solutes are added, the change in the SLD of the bulk solution would change the relative contrast of the hydration layer and the protein. This would cause the R_g inferred from Guinier plots to change with solute concentration even when the protein structure remained unchanged (8,13). In this section, we consider how a hydration layer would affect the apparent R_g as PEG is added to a solution of SOD. Our approach follows Stanley et al. (8) and Markovic et al. (40) in using a core-shell model to describe SOD and the presumed hydration layer.

R_g of a composite core-shell system, composed of protein (p) and water (w) is given by

$$R_g^2 = \frac{\Delta\rho_p V_p R_{g,p}^2 + \Delta\rho_w V_w R_{g,w}^2}{\Delta\rho_p V_p + \Delta\rho_w V_w}, \quad (2)$$

where V_p and $R_{g,p}$ are the volume and the radius of gyration of the protein, respectively. The values V_w and $R_{g,w}$ are the volume and the radius of gyration of the water layer, respectively. The value $\Delta\rho_p$ is the contrast of the protein with respect to bulk solution and is given by the difference between SLD of protein, ρ_p and SLD of the bulk solution, ρ_0, shown as $\Delta\rho_p = \rho_p - \rho_0$. The value $\Delta\rho_w$ is the contrast of the water layer with respect to bulk solution and is given by the difference in SLD of water, ρ_w and the bulk ρ_0, shown as $\Delta\rho_w = \rho_w - \rho_0$. The value ρ_0 will change as solute is added to solution. We assume ρ_0 is the weighted sum of ρ_w and ρ_s such that $\rho_0 = f_v\rho_s + (1 - f_v)\rho_w$, where f_v is the volume fraction of solute.

We evaluated Eq. 2 using parameters appropriate for SOD, PEG (dPEG in SANS and PEG in SAXS), and a presumed 3 Å water layer (D_2O in SANS and H_2O in SANS) for both SAXS and SANS. The SLDs, used in our calculations, are given in Table 1 and the geometrical parameters are given in Table 2, in the row labeled for Model *a*. Predicted values of R_g are shown in Fig. 10 *a*. The value R_g increases for SANS and decreases for SAXS with increased PEG concentration. This is inconsistent with the parallel decrease of R_g observed experimentally (Fig. 7).

SOD contains water at its dimer interface (14) and it could be argued that water occur as a core around which the protein forms a shell. We have also considered this case (Fig. 9 *b*; parameters given in Tables 1 and 2 in the row labeled for Model *b*). Predicted values of R_g decrease for SANS and increase for SAXS with increased %PEG. This is again inconsistent with the parallel decrease in R_g for SANS and SAXS observed experimentally.

It can readily be seen by expanding Eq. 2 about small f_v that R_g changes with added solutes in opposite directions for SANS and SAXS regardless of the particular geometry of the core-shell model. Explicitly,

$$R_g^2 = R_{g,0}^2 + \left.\frac{dR_g^2}{df_V}\right|_{f_v=0} f_v + \mathcal{O}(f_v^2), \quad (3)$$

TABLE 2 Fitting parameters for SOD-water models

Model	$R_{g,p}$(Å)	$R_{g,w}$(Å)	V_p(Å^3)	V_w(Å^3)
a	22.4	22.7	53,030	35,329
b	22.4	12.0	53,030	2543

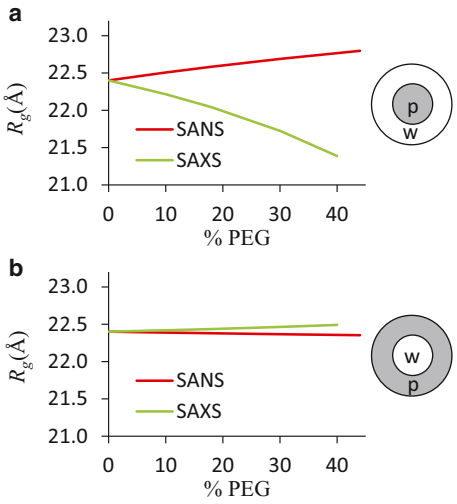

FIGURE 10 Core-shell model and its predictions for measured R_g as PEG (in SAXS) or dPEG (in SANS) is added to the solution. (*a*) For a protein core (*p*) surrounded by a water shell (*w*), R_g increases for SANS and decreases for SAXS. (*b*) For a water core (*w*) and a protein shell (*p*), R_g decreases for SANS and increases for SAXS. In SANS parameters for protonated SOD, dPEG and D_2O are used. In SAXS, parameters for SOD, PEG and H_2O are used. In our experiments we observed a decrease in R_g as a function of PEG% for both SANS and SAXS (Fig. 7). To see this figure in color, go online.

where $R_{g,0}{}^2$ is the R_g for $f_v = 0$ and

$$\left.\frac{dR_g^2}{df_V}\right|_{f_v=0} = \frac{\rho_w - \rho_s}{\rho_p - \rho_w}\frac{V_w}{V_p}\left(R_{g,w}^2 - R_{g,p}^2\right). \quad (4)$$

The ratio $(\rho_w - \rho_s)/(\rho_p - \rho_w)$ is positive for SANS and negative for SAXS. Therefore, changes in R_g due to a water layer when solutes are added will necessarily be in opposite directions for SANS and SAXS. However, we observed that R_g decreased in both SANS and SAXS (Fig. 7). Therefore, we conclude that the effects of a water layer on SAS from SOD is negligible.

ACKNOWLEDGMENTS

We thank Dr. Xiaobing Zuo at APS beamline 12-ID-B for his cheerful support during our SAXS experiment.

SAXS experiments were performed at the Advanced Photon Source of Argonne National Laboratory operated for the U.S. Department of Energy.

The research was supported by the National Science Foundation (grant No. 1006485-DMR). A portion of the research performed at Oak Ridge National Laboratory's Spallation Neutron Source was sponsored by the Scientific User Facilities Division, Office of Basic Energy Sciences, U.S. Department of Energy.

REFERENCES

1. Ellis, R. J. 2001. Macromolecular crowding: obvious but underappreciated. *Trends Biochem. Sci.* 26:597–604.
2. Ellis, R. J., and A. P. Minton. 2006. Protein aggregation in crowded environments. *Biol. Chem.* 387:485–497.
3. Minton, A. P. 2000. Implications of macromolecular crowding for protein assembly. *Curr. Opin. Struct. Biol.* 10:34–39.
4. Parsegian, V. A., R. P. Rand, and D. C. Rau. 2000. Osmotic stress, crowding, preferential hydration, and binding: a comparison of perspectives. *Proc. Natl. Acad. Sci. USA.* 97:3987–3992.
5. Street, T. O., K. A. Krukenberg, …, D. A. Agard. 2010. Osmolyte-induced conformational changes in the Hsp90 molecular chaperone. *Protein Sci.* 19:57–65.
6. Eggers, D. K., and J. S. Valentine. 2001. Molecular confinement influences protein structure and enhances thermal protein stability. *Protein Sci.* 10:250–261.
7. Sasahara, K., P. McPhie, and A. P. Minton. 2003. Effect of dextran on protein stability and conformation attributed to macromolecular crowding. *J. Mol. Biol.* 326:1227–1237.
8. Stanley, C., S. Krueger, …, D. C. Rau. 2008. Protein structure and hydration probed by SANS and osmotic stress. *Biophys. J.* 94:2777–2789.
9. Konarev, P. V., V. V. Volkov, …, D. I. Svergun. 2003. PRIMUS: a windows PC-based system for small-angle scattering data analysis. *J. Appl. Cryst.* 36:1277–1282.
10. Jacques, D. A., and J. Trewhella. 2010. Small-angle scattering for structural biology—expanding the frontier while avoiding the pitfalls. *Protein Sci.* 19:642–657.
11. Timasheff, S. N. 2002. Protein hydration, thermodynamic binding, and preferential hydration. *Biochemistry.* 41:13473–13482.
12. Svergun, D. I., S. Richard, …, G. Zaccai. 1998. Protein hydration in solution: experimental observation by x-ray and neutron scattering. *Proc. Natl. Acad. Sci. USA.* 95:2267–2272.
13. Murthy, N. S., and J. R. Knox. 2004. Hydration of proteins: SAXS study of native and methoxy polyethyleneglycol (mPEG)-modified L-asparaginase and bovine serum albumin in mPEG solutions. *Biopolymers.* 74:457–466.
14. Rodier, F., R. P. Bahadur, …, J. Janin. 2005. Hydration of protein-protein interfaces. *Proteins.* 60:36–45.
15. Yost, Jr., F. J., and I. Fridovich. 1973. An iron-containing superoxide dismutase from *Escherichia coli*. *J. Biol. Chem.* 248:4905–4908.
16. Miller, A. F. 2012. Superoxide dismutase: ancient enzymes and new insights. *FEBS Lett.* 586:585–595.
17. Beauchamp, C., and I. Fridovich. 1971. Superoxide dismutase: improved assays and an assay applicable to acrylamide gels. *Anal. Biochem.* 44:276–287.
18. McCord, J. M., and I. Fridovich. 1969. Superoxide dismutase. An enzymic function for erythrocuprein (hemocuprein). *J. Biol. Chem.* 244:6049–6055.
19. Janknegt, P. J., J. W. Rijstenbil, …, A. G. J. Buma. 2007. A comparison of quantitative and qualitative superoxide dismutase assays for application to low temperature microalgae. *J. Photochem. Photobiol. B.* 87:218–226.
20. Arnold, O., J. C. Bilheux, …, J. Zikovsky. 2014. MANTID—data analysis and visualization package for neutron scattering and mu-SR experiments. *Nucl. Instrum. Methods Phys. Res. A.* A764:156–166.
21. Svergun, D. I. 1992. Determination of the regularization parameter in indirect-transform methods using perceptual criteria. *J. Appl. Cryst.* 25:495–503.
22. Svergun, D. I., M. H. J. Koch, …, R. P. May. 2013. Small angle x-ray and neutron scattering from solutions of biological macromolecules. *In* IUCr Texts on Crystallography, *Vol. 19*. Oxford University Press, New York.
23. Lah, M. S., M. M. Dixon, …, M. L. Ludwig. 1995. Structure-function in *Escherichia coli* iron superoxide dismutase: comparisons with the manganese enzyme from *Thermus thermophilus*. *Biochemistry.* 34:1646–1660.
24. Harries, D., and J. Rösgen. 2008. A practical guide on how osmolytes modulate macromolecular properties. *Methods Cell Biol.* 84:679–735.
25. Money, N. P. 1989. Osmotic pressure of aqueous polyethylene glycols' relationship between molecular weight and vapor pressure deficit. *Plant Physiol.* 91:766–769.
26. Guinier, A. 1963. X-Ray Diffraction. Freeman, San Francisco, CA.

27. O. Glatter, and O. Kratky, editors 1982. Small Angle X-Ray Scattering. Academic Press, London, United Kingdom.

28. Svergun, D. I., and M. H. J. Koch. 2003. Small-angle scattering studies of biological macromolecules in solution. *Rep. Prog. Phys.* 66:1735–1782.

29. Tait, M. J., and F. Franks. 1971. Water in biological systems. *Nature.* 230:91–94.

30. Kuntz, Jr., I. D., and W. Kauzmann. 1974. Hydration of proteins and polypeptides. *Adv. Protein Chem.* 28:239–345.

31. Windsor, C. G. 1988. An introduction to small-angle neutron scattering. *J. Appl. Cryst.* 21:582–588.

32. Eggers, D. K., and J. S. Valentine. 2001. Crowding and hydration effects on protein conformation: a study with sol-gel encapsulated proteins. *J. Mol. Biol.* 314:911–922.

33. van den Berg, B., R. J. Ellis, and C. M. Dobson. 1999. Effects of macromolecular crowding on protein folding and aggregation. *EMBO J.* 18:6927–6933.

34. Miyoshi, D., A. Nakao, and N. Sugimoto. 2002. Molecular crowding regulates the structural switch of the DNA G-quadruplex. *Biochemistry.* 41:15017–15024.

35. van den Berg, B., R. Wain, …, R. J. Ellis. 2000. Macromolecular crowding perturbs protein refolding kinetics: implications for folding inside the cell. *EMBO J.* 19:3870–3875.

36. Schnell, S., and T. E. Turner. 2004. Reaction kinetics in intracellular environments with macromolecular crowding: simulations and rate laws. *Prog. Biophys. Mol. Biol.* 85:235–260.

37. Zhou, H.-X., G. Rivas, and A. P. Minton. 2008. Macromolecular crowding and confinement: biochemical, biophysical, and potential physiological consequences. *Annu. Rev. Biophys.* 37:375–397.

38. Fridovich, I. 1975. Superoxide dismutases. *Annu. Rev. Biochem.* 44:147–159.

39. Leikin, S., D. C. Rau, and V. A. Parsegian. 1994. Direct measurement of forces between self-assembled proteins: temperature-dependent exponential forces between collagen triple helices. *Proc. Natl. Acad. Sci. USA.* 91:276–280.

40. Markovic, I., R. H. Ottewill, …, J. F. Marsh. 1984. Small angle neutron scattering studies on non-aqueous dispersions of calcium carbonate. *Colloid Polym. Sci.* 262:648–656.

41. Munter, A. 2014. Scattering length density (SLD) calculator. http://www.ncnr.nist.gov/resources/sldcalc.html.